Hindered Diffusion of Water-Soluble Macromolecules in Membranes

Marc G. Davidson and William M. Deen*

Department of Chemical Engineering, Massachusetts Institute of Technology, Cambridge, Massachusetts 02139. *Received February 16, 1988; Revised Manuscript Received May 11, 1988*

ABSTRACT: The diffusion coefficients of four water-soluble macromolecules were determined in membranes containing pores having dimensions comparable to those of the solutes. The effective diffusion coefficients of ficoll, a highly cross-linked polysaccharide, were in excellent agreement with those predicted by a hydrodynamic theory for a solid, spherical solute. Effective diffusion coefficients for linear poly(ethylene oxide) (PEO) were between those predicted for a solid sphere and for a flexible, linear polymer. In contrast, linear poly(vinylpyrrolidone) (PVP) and nearly linear dextran diffused through the membranes more rapidly than predicted by either theory. The observed hindered diffusion behavior of dextran, PEO, and PVP is consistent with the relative behavior of these macromolecules on size-exclusion chromatographic columns and can be explained by moderate, attractive interactions between the polymers and the pore wall. The effects of polymer adsorption and polydispersity on hindered diffusion measurements are considered.

Introduction

The effective diffusion coefficient of a solute within a pore of comparable size is usually lower than its bulk solution value. This phenomenon, known as "hindered" or "restricted" diffusion, results from hydrodynamic and entropic restrictions on the solute due to the presence of the pore wall and arises in such areas as membrane separations and heterogeneous catalysis.

Several theoretical studies of hindered diffusion through porous membranes have been based on a hydrodynamic approach in which the membrane is treated as an array of cylindrical pores. The characteristic radii of the solute and pore are assumed to be comparable to one another but much larger than that of the solvent. This latter assumption allows application of the Stokes–Einstein equation, relating the diffusion coefficient of a solute in an infinitely dilute bulk solution, D_∞, to the Stokes–Einstein radius of the solute, r_s:

$$D_\infty = \frac{kT}{6\pi\eta r_s} \tag{1}$$

where k is Boltzmann's constant, T is absolute temperature, and η is the solvent viscosity.

When the solute is confined to a pore its apparent diffusion coefficient (based on concentrations external to the membrane) is reduced by two factors: steric exclusion from the region near the pore wall and increased hydrodynamic drag on the solute. Various results for the effective diffusion coefficient (D) of a solute through pores of radius r_p[1-4] can be summarized by

$$D/D_\infty \approx \Phi K^{-1} \tag{2}$$

In eq 2, Φ is the partition coefficient, or ratio of the average solute concentration within the pore to that in bulk solution, and accounts for steric exclusion (as well as long-range interactions if present). K^{-1} is the inverse enhanced drag, or ratio of the friction coefficient of the solute in bulk solution to that within the pore, and accounts for the increased hydrodynamic resistance to solute motion. The ratio D/D_∞ is often referred to as the hindrance factor for diffusion. For an uncharged, solid, spherical solute of radius r_s the effective diffusion coefficient can be expressed compactly in terms of the solute-to-pore size ratio λ (= r_s/r_p) by the Renkin equation:[1]

$$D/D_\infty \approx (1-\lambda)^2(1 - 2.1044\lambda + 2.089\lambda^3 - 0.948\lambda^5) \tag{3}$$

In eq 3 $\Phi = (1-\lambda)^2$, and the remaining term is an approximation to K^{-1} suitable for $\lambda \leq 0.4$. Various other hydrodynamic theories of hindered transport, including other expressions for K^{-1} of solid spheres, have been reviewed recently.[4]

Recently, we developed a hydrodynamic theory for the hindered transport of linear random-coiling macromolecules.[3] Because the Stokes–Einstein radius does not uniquely determine the physical dimensions of the polymer coil, the hindrance behavior predicted by our model depends on a dimensionless parameter α, in addition to λ. The parameter α, which is inversely related to the permeability of the coil to solvent, relates the Stokes–Einstein radius to the radius of gyration (r_g) of the coil. The value of α depends on the polymer–solvent system of interest (including polymer molecular weight). However, for a given polymer α tends to decrease as the polymer coil expands with increasing solvent quality.

The hydrodynamic behavior of the coil is determined primarily by r_s (and not r_g). Therefore, the dependence of the enhanced drag on α is relatively weak, and K^{-1} can be approximated by

$$K^{-1} = 1 - 2.848\lambda + 3.269\lambda^2 - 1.361\lambda^3 \tag{4}$$

for $\lambda \leq 0.87$ (see Appendix A). The partition coefficient of a random coil depends most directly on the ratio of the radius of gyration of the coil to the pore radius λ_g (=r_g/r_p), which can be related to λ and α by[3]

$$\frac{\lambda_g}{\lambda} = \frac{3(3^{1/2})}{2}\,\frac{\alpha + 5.77}{2.22\alpha} \tag{5}$$

Typically, the permeability parameter is in the range $10 \leq \alpha \leq 60$,[3] so that $1.3 \leq \lambda_g/\lambda \leq 1.8$. In many cases of interest, the partition coefficient of a neutral, random-coiling macromolecule can be approximated by the analytical expression of Casassa[5] for Φ of a freely jointed chain with an infinite number of infinitesimally short segments

$$\Phi = 4\sum_{i=1}^{\infty}(1/d_i^2)\exp(-d_i^2\lambda_g^2) \tag{6}$$

where d_i are the roots of $J_0(d) = 0$, J_0 representing the Bessel function of the first kind, of order zero. By combining this result with eq 4, our theoretical results for the hindered diffusion coefficient of a random coil can be reasonably approximated (see Appendix A for details). A similar approximate expression for the hindrance factor for convection is described in Appendix A.

Track-etched membranes, which have simple and well-defined pore geometries, provide opportunities for

* Author to whom correspondence should be addressed.

0024-9297/88/2221-3474$01.50/0

quantitative tests of theories of hindered diffusion.[4] These membranes have been used to study the hindered diffusion of proteins,[6,7] polysaccharides,[8,9] and linear[10-13] and star-branched[13] synthetic polymers. It was the purpose of this study to investigate further the effects of pore size and molecular configuration on the hindered diffusion of water-soluble polymers in track-etched membranes. To this end, the hindered diffusion of four polymers in water was studied: dextran, a nearly linear polysaccharide; ficoll, a highly cross-linked polysaccharide; and poly(ethylene oxide) (PEO) and poly(vinylpyrrolidone) (PVP), both linear synthetic polymers. All of these water-soluble macromolecules have been used previously to study the selectivity of biological membranes.[14-16]

Experimental Section

Polymer Fractionation and Characterization. Dextran T70 (lot 8027) and ficoll 70 (lot 13902) with weight-averaged molecular weights of approximately 70 000 (M_w/M_n = 1.6 and 1.9, respectively) were obtained from Pharmacia Fine Chemicals (Piscataway, NJ). Each of these polymer samples was fractionated twice on a Sephacryl S-300 (Pharmacia) gel column (2.6 cm × 61 cm) using 0.02 M ammonium acetate as the eluent. Eluent was pumped at 1.0 mL/min. For the first fractionation, 0.2 g of polymer in 2 mL of eluent was applied to the column, and 15 mL centered at the peak polymer concentration was collected and freeze-dried. For the second fractionation 0.1 g of the polymer dissolved in 2 mL of eluent was applied to the column, and 20-mL fractions were collected. The twice-fractionated polymer was extensively freeze-dried to remove any residual ammonium acetate.

Poly(vinylpyrrolidone) (PVP) with nominal molecular weight of 40 000 ($M_w/M_n \approx 3$) was obtained from Scientific Polymer Products (Ontario, NY) (lot 16) and fractionated by sequential precipitations using water as the solvent and acetone as the nonsolvent. The first fractionations were conducted with 3.0 g of PVP dissolved in 80 mL of water. In a 500-mL separatory funnel, 250 mL of acetone was added to the polymer solution under mild agitation. The mixture was allowed to equilibrate for 3 days at room temperature, at which time the lower phase (containing the higher molecular weight polymer) was removed. To the remaining phase, 100 mL of acetone was added under agitation, and the mixture was allowed to equilibrate for at least 5 days. The lower phase was then removed and freeze-dried. The second fractionation, using 2.4 g of once-fractionated PVP, was identical with the first except that the acetone additions were 350 and 50 mL, respectively.

A poly(ethylene oxide) (PEO) sample, with weight-averaged molecular weight 21 000, was obtained from Toyo Soda (Varian Associates, Sunnyvale, CA). This sample had a narrow molecular weight distribution (M_w/M_n = 1.12) and did not require fractionation.

The four polymer samples were characterized by using quasi-elastic light scattering on a Coulter Electronics (Hialeah, FL) System N4 submicron particle analyzer. Concentrations below $0.25/[\eta]$ (where $[\eta]$ is the intrinsic viscosity) were used to minimize interactions between polymer molecules. The mean dilute solution diffusion coefficient D_∞ in water at 25 °C, the mean Stokes–Einstein radius r_s, and the standard deviation of the Stokes–Einstein radius σ_s were obtained by using the method of constrained regularization.[17]

Membrane Characterization. Track-etched polycarbonate membranes with nominal pore radii of 15, 25, and 50 nm were obtained from Nuclepore Corp. (Pleasanton, CA). These membranes contain pores which are uniform, circular cylinders. The average pore length is slightly larger than the membrane thickness because the pores are not aligned exactly perpendicular to the membrane surface. Assuming all deviations from the normal are equally probable up to the maximum deviation of 29° (information from Nuclepore), the average pore length will exceed the membrane thickness by 6.8% and is given by

$$L = \frac{1.068 W_m}{(1 - n\pi r_p^2) A \rho_m} \tag{7}$$

where W_m is the mass of the membrane, A is the total membrane area (14.5 cm^2), and ρ_m is the density of polycarbonate (1.19 g/cm^3). The term in parentheses is a correction for the membrane porosity, where n and r_p are the number density of pores and the pore radius, respectively.

The number density of pores for each membrane lot was determined by counting the number of pores in scanning electron micrographs of known area. An International Scientific Instruments (Santa Clara, CA) Model DS1300 scanning electron microscope was used at 15 000–20 000× magnification. Each photograph contained 80–200 pores, and at least 12 photographs were taken for each membrane lot.

Water flow measurements were used to determine the pore radii for each membrane. The membrane was mounted in an Amicon (Lexington, MA) Model 52 ultrafiltration cell. A constant transmembrane flow rate (Q) was produced by using a Sage Instruments (Cambridge, MA) Model 341A syringe pump, and the resulting transmembrane pressure drop (ΔP) was measured by using a Validyne Engineering (Northridge, CA) Model DP15 pressure transducer. The Poiseuille equation was used to obtain the pore radius (r_p):

$$r_p = \left(\frac{8\eta L Q}{n\pi A_u \Delta P} \right)^{1/4} \tag{8}$$

where A_u is the exposed membrane area in the ultrafiltration cell. Water flow measurements were performed at room temperature (22 ± 3 °C). Measurements were taken at two flow rates between 1.7 and 9.7 mL/h for each membrane. Within this range, there was no detectable effect of flow rate on hydraulic permeability. The pore Reynolds number was never greater than 5 × 10^{-6}.

Test for Polymer Adsorption. Polymer adsorption, if significant, can complicate interpretation of hindered diffusion data by reducing effective membrane pore radii. To consider this possibility, we performed a separate study using the water flow technique described above. Flow measurements were performed on four membranes with nominal pore radii of 15 nm. Each of these membranes was then immersed in a bath of polymer solution at room temperature for 72 h. The polymer solutions (0.05 g/100 mL) were prepared from unfractionated polymer dissolved in distilled water. A higher molecular weight PEO sample (M_w = 45 000) was used to study PEO adsorption. After incubation, the membranes were rinsed in distilled water and subjected to a second set of flow measurements.

The results are presented in Table I in terms of the quantity $\eta Q/\Delta P$, which should remain unchanged if polymer adsorption is insignificant. The results of the study indicated that adsorption of dextran and ficoll is negligible. For both dextran[18,19] and ficoll[18] in dilute solution, this conclusion is supported by previous water flow measurements. In contrast, both PEO and PVP adsorb to the membranes, resulting in large reductions in the quantity $\eta Q/\Delta P$. These reductions correspond to a 34% and 25% reduction in the pore radius for PEO and PVP, respectively. When these membranes were soaked in distilled water for 20–40 h and water flow measurements repeated, relatively small increases in $\eta Q/\Delta P$ were observed, reflecting a small degree of desorption. Because adsorption of these polymers complicates the measurement and

Table I
Water Flow Results on Membranes before and after Exposure to Polymer

membrane	treatment	$\eta Q/\Delta P$, 10^{-9} cm^3	% change[b]
1	none	1.22	
	dextran	1.15	−5.6
2	none	1.25	
	ficoll	1.37	+2.3
3	none	1.37	
	PEO	0.26	−80.9
	water[a]	0.41	−70.0
4	none	1.24	
	PVP	0.40	−68.1
	water[a]	0.55	−56.0

[a] Membrane 3 was soaked in distilled water for 40 h after exposure to PEO. Membrane 4 was soaked in distilled water for 22 h after exposure to PVP. [b] Percent change from original $\eta Q/\Delta P$ value.

interpretation of their hindered diffusion behavior, the procedures used to obtain and evaluate PEO and PVP hindered diffusion data are discussed separately below.

Pretreatment of Membranes with Adsorbing Polymers. Membranes used to study PEO and PVP hindered diffusion were pretreated by soaking them in 0.05 g/100 mL solutions of the polymer to be used in the diffusion experiments. Limited kinetic studies, monitoring hydrodynamic thickness of the adsorbed layer periodically by water flow measurements, indicated that PEO adsorption equilibrium had been reached after approximately 24 h. PVP adsorption was slower, the hydrodynamic thickness reaching roughly 65% of its equilibrium value after 1 day and 80% after 4 days. All membranes used with PEO and PVP were allowed to equilibrate for at least 4 days prior to their use in diffusion experiments. Water flow measurements were performed on these membranes immediately before and after each hindered diffusion experiment.

Hindered Diffusion Measurements. Diffusion experiments were performed by using a Lucite diffusion cell similar to those used in previous studies.[8,9] The cell consisted of two identical half-cells each having a volume (V) of 20.6 cm^3. The membrane was mounted between two annular disks which were clamped between the half-cells. The exposed membrane area (A_d) was 7.92 cm^2. Each half-cell contained a Teflon-coated magnetic stirring disk mounted on a stainless steel shaft. The stirring disks were rotated at 200 ± 30 rpm by an external magnet. The temperature of the cell was controlled by a water jacket maintained at 25.0 ● 0.1 °C.

The difference in concentration between the two half-cells was measured periodically by drawing approximately 1 mL of solution from one of the chambers and recording its refractive index relative to pure solvent by using a Waters Associates (Milford, MA) Model R403 differential refractometer. Measurement of the refractive index of the solutions on both sides of the membrane required approximately 3 min. Each half-cell was kept closed except during sampling. Neglecting adsorption and desorption, the concentration difference between the two half-cells (ΔC) is required by conservation of mass to follow the relation

$$\ln\left(\frac{\Delta C}{\Delta C_0}\right) = -\frac{2A_d t}{VR_T} \tag{9}$$

where ΔC_0 is the initial concentration difference, R_T is the total mass transfer resistance, and t is time. The solute diffusion coefficient in the membrane, D, is related to the total mass transfer resistance (R_T) by

$$R_T = \frac{L}{n\pi r_p^2 D} + R_B \tag{10}$$

In eq 10, the first term on the right-hand side represents the membrane resistance and R_B represents the boundary layer resistance. (For the membranes and polymers of interest, the correction for the fact that diffusion is not one-dimensional near the membrane surface[20] is negligible.) The boundary layer resistance for each membrane was determined by measuring the diffusion of sucrose across the membrane. Although the sucrose molecule is much smaller than any of the pore radii, the Renkin equation predicts that D will be reduced by 2–10%, and such reductions are in agreement with available data.[4] Accordingly, in determining R_B from eq 10, D for sucrose was estimated by using eq 3. A correlation of the form developed by Colton and Smith[21] for this geometry yields

$$R_B \propto D_\infty^{-1}\mathrm{Sc}^{-1/3} \tag{11}$$

where Sc ($=\eta/\rho D_\infty$, with ρ the solvent density) is the Schmidt number. From this relation we can estimate the R_B value for the polymeric solute as

$$R_{B,\text{polymer}} = R_{B,\text{sucrose}}\left[\frac{D_{\infty,\text{sucrose}}}{D_{\infty,\text{polymer}}}\right]^{2/3} \tag{12}$$

The procedure for diffusion experiments was as follows. Initially, one half-cell was filled with distilled water and the other with dilute (0.04 g/100 mL) polymer solution. The slope of a plot of the resulting ln ($\Delta C/\Delta C_0$) versus t data was determined by linear regression. The time required for each hindered diffusion experiment varied between 10 and 70 h depending on the size of the membrane pores and the macrosolute. In most cases, the experiment was allowed to run at least until the concentration difference across the membrane had dropped to half its initial value. At least one experiment was allowed to continue until $\Delta C/\Delta C_0 < 0.25$ for each polymer studied. The reproducibility of individual data points may be judged from the observation that, in preliminary experiments (with incompletely characterized membranes), duplicate diffusion experiments with the same polymer–membrane combination yielded D/D_∞ values within 12% of each other.

Since the hindered diffusion rates are extremely sensitive to solute size, the polydispersity of the polymer samples might have a significant effect on the results. To account for possible polydispersity effects, we have developed an approximate correction, assuming a normal distribution of solute sizes and solid sphere hindrance behavior. The details of the polydispersity correction and a discussion of simulated polydispersity effects are provided in Appendix B. The analysis predicts that allowing the concentration difference to drop to roughly one-third of its original value, as we have done, minimizes the error due to polydispersity.

Table II
Characteristics of Macromolecules in Water at 25 °C

polymer	D_∞, 10^{-7} cm^2/s	r_s, nm	σ_s, nm
dextran	4.5	5.5	1
ficoll	7.0	3.5	1
PEO	5.6	4.4	1
PVP	4.4	5.6	2

Results

The results of the quasi-elastic light scattering are shown in Table II. The four polymer samples had bulk solution diffusivities of (4.4–7.0) × 10^{-7} cm^2/s and mean Stokes–Einstein radii from 3.5 to 5.6 nm. The dextran and ficoll samples had estimated standard deviations in solute size equal to that of the PEO sample (σ_s = 1), suggesting the polydispersity indices of the fractionated dextran and ficoll are comparable to that of PEO (M_w/M_n = 1.12). The PVP sample had an estimated σ_s value twice that of the other three polymer samples, indicating a higher degree of polydispersity. This result is reasonable considering that the unfractionated PVP was considerably more polydisperse than dextran and ficoll ($M_w/M_n \approx 3$ for PVP, versus 1.6 and 1.9 for dextran and ficoll, respectively).

The membrane characterization results are summarized in Table III. Pore radii and lengths were measured for each membrane, while pore number densities were assumed to be the same for all membranes in a particular lot. The estimated error in the pore radii, pore lengths, and number densities is 3%, 2%, and 8%, respectively. As in other investigations,[18,22] we found that while the pore lengths were very close to the nominal value of 6 μm the number densities and pore radii exceeded their nominal values by up to 50% and 70%, respectively. (The nominal pore densities are 3 × 10^8 cm^{-2} for the 50-nm nominal pore radii membranes and 6 × 10^8 cm^{-2} for the 15- and 25-nm nominal pore radii membranes.) For membranes used to study PEO and PVP diffusion, the original pore radii (before pretreatment) and the average of the pore radii determined immediately before and after the diffusion run are included in Table III. The pore radii calculated from water flow measurements before and after the diffusion experiment never differed by more than 3%, indicating negligible changes in the thickness of the adsorbed layer during the hindered diffusion run. The estimated hydrodynamic thicknesses of adsorbed polymer, or the difference between the original and final pore radii, were 6–7 nm for PEO and 3–6 nm for PVP.

Table III
Properties of Track-Etched Membranes

nominal pore radius, nm	polymer exposure	r_p,[a] nm	n, 10^8 cm^{-2}	L, μm
50	dextran, ficoll	59.7	4.56	6.26
	PEO	52.8		6.21
		(60.5)		
	PVP	53.2		6.15
		(59.4)		
25	dextran, ficoll	34.4	9.05	6.19
	PEO	28.8		6.04
		(34.8)		
	PVP	32.0		6.06
		(35.0)		
15	dextran	25.2	7.69	6.59
	ficoll	26.5		6.48
	PEO	19.7		6.19
		(26.3)		
	PVP	23.7		6.47
		(26.5)		

[a] For membranes exposed to PEO and PVP, reported pore radii are the average of pore radii measured by water flow immediately before and after hindered diffusion experiment. Pore radii prior to exposure to polymer are given in parentheses.

Table IV
Hindrance Factors for Diffusion: Uncorrected and Corrected for Polydispersity

		D/D_∞	
polymer	$\bar{\lambda}$[a]	uncorrected	corrected
dextran	0.092	0.83	0.82
	0.16	0.67	0.66
	0.22	0.46	0.45
ficoll	0.058	0.82	0.80
	0.10	0.64	0.65
	0.13	0.58	0.56
PEO	0.083	0.68	0.68
	0.15	0.47	0.45
	0.22	0.29	0.27
PVP	0.10	0.88	0.88
	0.17	0.54	0.56
	0.23	0.52	0.49

[a] Values of $\bar{\lambda}$ for PEO and PVP are based on the average of pore radii measured by water flow immediately before and after the hindered diffusion experiment.

The hindered diffusion experiments produced the expected exponential decay in ΔC. Linear regressions according to eq 9 had high correlation coefficients, with $r^2 > 0.99$ in most cases. Except for runs with PEO, regressions which included the polydispersity correction had slightly better correlation coefficients, suggesting that the correction was useful in reducing any nonlinearities due to polydispersity effects. Boundary layer resistances were typically about 20%, 8%, and 3% of the total mass transfer resistance for the 50-, 25-, and 15-nm nominal pore radii membranes, respectively.

The hindered diffusion data for the four water-soluble polymers are presented in Table IV and in Figure 1 in terms of the mean solute-to-pore size ratio $\bar{\lambda}$ and the ratio of the diffusion coefficient in the membrane relative to that in bulk solution, D/D_∞. The reported $\bar{\lambda}$ values for PEO and PVP are based on water flow measurements after presoaking the membranes. Also shown in Figure 1 are the theoretical results for a solid sphere (eq 3) and for a random-coiling polymer (eq 2, 4, and 6 with $\alpha = 34$). As can be seen, the data for ficoll, the highly cross-linked polysaccharide, follow eq 3 quite closely. The dextran and PVP data lie well above both theoretical curves. In contrast to these linear (or nearly linear) polymers, the data for PEO fall between the theoretical curves for a random coil and a solid sphere. The polydispersity correction

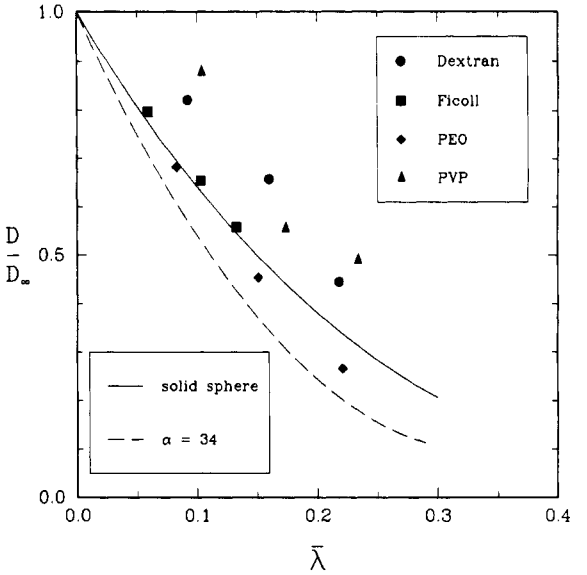

Figure 1. Effective diffusion coefficient in the membrane relative to that in bulk solution, D/D_∞, versus mean solute-to-pore size ratio $\bar{\lambda}$. Symbols represent data corrected for polydispersity. The solid line is behavior predicted for a solid, spherical solute. The dashed line is behavior predicted for a noninteracting, linear macromolecule ($\alpha = 34$).

produced only minor changes in the calculated D/D_∞ values, as shown in Table IV. It should be noted that the corrections for polydispersity are small because the final concentration differences in the experiments were in the range that minimizes polydispersity effects. When the final value of $\Delta C/\Delta C_0$ was higher than roughly 0.24, the polydispersity correction yielded a lower value of D/D_∞. Conversely, final $\Delta C/\Delta C_0$ values below 0.24 resulted in higher values of D/D_∞ in most cases. Because the correction never changed D/D_∞ by more than 0.03, only the corrected values are shown in Figure 1.

Discussion

As stated earlier, the adsorption of PEO and PVP to the membrane pores complicates interpretation of the hindered diffusion data. The strong effect of pore size on hindered diffusion behavior in this study demonstrates the importance of accounting for polymer adsorption. In evaluating the data presented here we have assumed that the appropriate effective pore radii are those determined by water flow measurements after adsorption. However, the hydrodynamic thickness of the adsorbed layer will depend on the density and distribution of adsorbed polymer within the adsorbed layer.[23] In a number of recent investigations, the effects of adsorption of flexible[24,25] and rigid[18,26] macromolecules on solvent and solute transport through pores have been considered. More work is needed to understand hindered transport in pores containing substantial layers of adsorbed polymers. Nonetheless, the approach taken here is consistent in that, as manufactured, all of the membranes contain some adsorbed PVP to facilitate wetting.

While the effective diffusion coefficient of all of the water-soluble polymers studied decreased with decreasing pore size, the strength of this pore size dependence varied from polymer to polymer. The close fit of the ficoll data to the Renkin equation suggests that it behaves much like a solid sphere. This result is in excellent agreement with that of Bohrer et al.,[9] who reported similar results for ficoll up to $\bar{\lambda} = 0.6$. In addition, our dextran hindered diffusion data, which fall well above the theoretical predictions, are in good agreement with those reported in that study. In

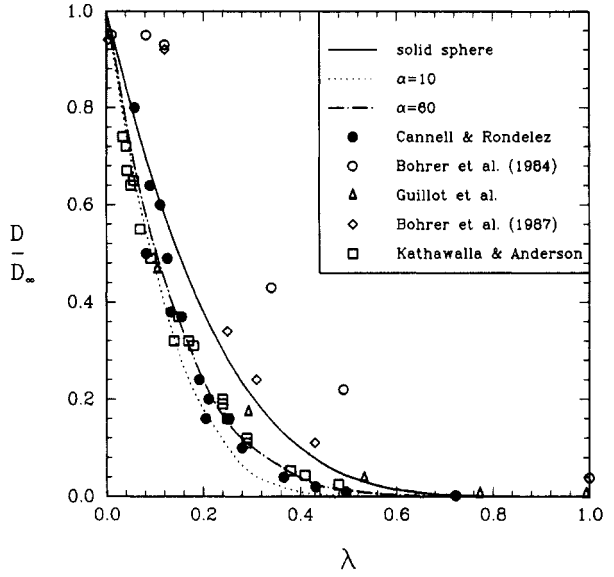

Figure 2. Comparison of experimental hindered diffusion data with theoretical predictions for random-coiling macromolecules (α = 10 and 60) and for a solid, spherical solute. The data are for the following polymer/solvent systems: Cannell and Rondelez[10] and Guillot et al.,[11] polystyrene/ethyl acetate; Kathawalla and Anderson,[12] polystyrene/tetrahydrofuran; Bohrer et al. (1984),[9] dextran/water; Bohrer et al. (1987),[13] polyisoprene/*n*-amyl acetate. Kathawalla and Anderson[12] used track-etched mica membranes, while Bohrer et al.[13] used both polycarbonate and polyester membranes. Track-etched polycarbonate membranes were used in all of the other studies.

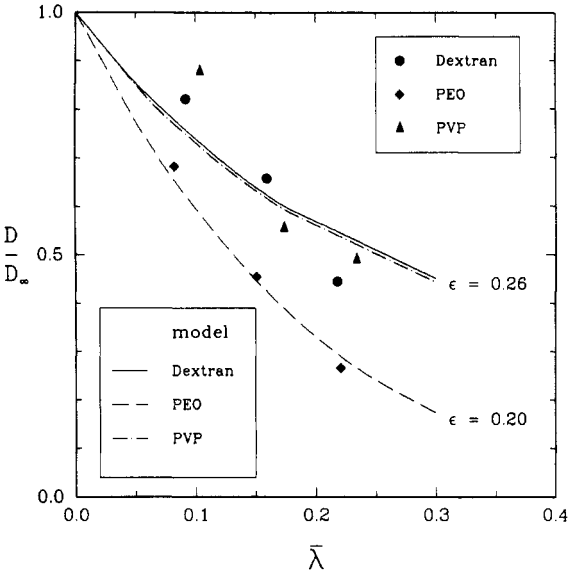

Figure 3. Comparison of experimental D/D_∞ data with the model for a linear macromolecule with attractive polymer–pore interactions. The values of the dimensionless, attractive interaction energy ϵ providing the best fit were 0.26 for dextran and PVP and 0.20 for PEO.

an earlier investigation, Deen et al.[8] also found D/D_∞ for dextran to be larger than that of ficoll at the same value of $\bar{\lambda}$.

To date, there have not been any other investigations of either PEO or PVP hindered diffusion in track-etched membranes. However, there have been a number of studies using other linear polymers. Data from these studies are compared to the theoretical predictions for spheres and random-coiling macromolecules in Figure 2. Data for linear polystyrene in ethyl acetate[10,11] and in tetrahydrofuran[12] are in good agreement with our theoretical predictions for a random-coiling polymer, and thus polystyrene is hindered to a greater extent than either PEO or PVP when compared at the same $\bar{\lambda}$ value. In contrast, available D/D_∞ data for linear polyisoprene in *n*-amyl acetate[13] lie slightly above the values predicted by the Renkin equation. (In this same investigation, star-branched polyisoprenes had D/D_∞ values well below theoretical predictions for branched and linear polymers.) As can be seen, even among linear macromolecules a wide range of hindered diffusion behavior has been observed.

Attractive polymer–pore interactions might be responsible for observed effective diffusion coefficients which are considerably higher than predicted for a noninteracting random coil.[3] Using a model of partitioning, in which segments of the polymer chain within one segment length of the pore wall are attracted with an interaction energy of ϵkT, we demonstrated that significant increases in the partition coefficient occur when moderate ($0.1 < \epsilon < 0.3$) attractive interaction energies are included.[27] It should be noted that adsorption of the polymer coil will occur only if ϵ is above some threshold value. For positive values of ϵ below this threshold, the polymer molecule is merely attracted toward the pore surface. (In this context, the "pore surface" includes any preadsorbed polymer layer present.) We have applied this partitioning model, in combination with the hydrodynamic calculations for a random coil, to estimate the interaction energies required to produce the hindered diffusion behavior observed for dextran, PEO, and PVP. Assuming each polymer segment to correspond to a monomer, we used literature data on D_∞ versus molecular weight[28-30] to determine the number of segments for the polymer samples used in this study. The number of segments was found to be 310, 540, and 460 for dextran, PEO, and PVP, respectively. With these values and assuming α = 40 (found to be an appropriate value for the dextran sample), ϵ was varied to obtain a best fit to the hindered diffusion data for each polymer. The dimensionless interaction energies (ϵ) providing the best fit were 0.26 for dextran and PVP and 0.20 for PEO. The model behavior using these values of the interaction energy is compared with the data in Figure 3. While the model is able to reproduce the behavior of PEO very accurately, it is unable to capture the curvature in the dextran and PVP data. This may be due in part to scatter in the data. The exact values of ϵ are of little significance, primarily because of the crudeness of the assumed square-well potential. However, it is apparent from this analysis that the existence of moderate, attractive polymer–pore interactions would result in D/D_∞ values of the magnitude observed experimentally.

The adsorption of PVP and PEO to the membranes is strong evidence that attractive polymer–pore interactions are occurring in these systems. Further evidence of polymer–pore interactions is provided by an investigation of size-exclusion chromatography (SEC) of dextran, PEO, and PVP on columns containing cross-linked dextran (Sephadex) packing.[31] In that study dextran and PVP had elution times considerably longer than those of PEO of the same size, based on the "universal calibration" parameter $[\eta]M_w$. The longer elution times indicate that the dextran and PVP were able to access the pore volume of the packing material with relative ease and as a result had higher partition coefficients. This finding is consistent with the hindered diffusion behavior of these three polymers observed in this study. Because SEC is performed at near-equilibrium conditions, it supports our belief that the discrepancy between predicted and observed hindered diffusion behavior results primarily from partitioning (rather than hydrodynamic) effects. In addition, the trends observed, relative to dextran, for the filtration of ficoll,[14]

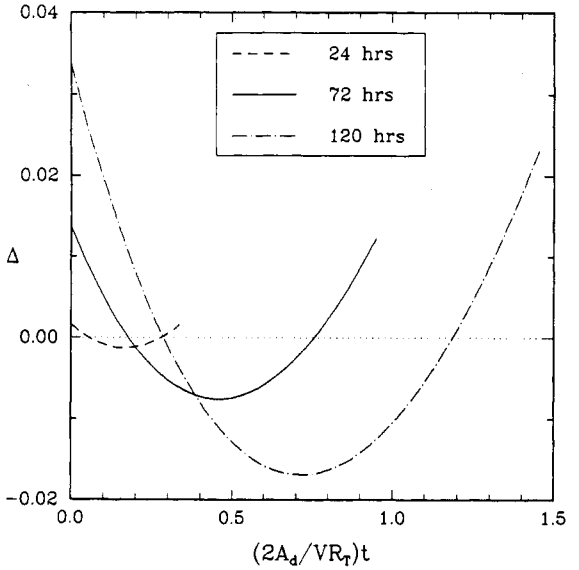

Figure 4. Simulated residuals Δ versus dimensionless time $(2A_d/VR_T)t$ for hindered diffusion runs of 24, 72, and 120 h, sampling concentrations every 4 h. Parameters typical of experiments with 15-nm nominal pore radius membranes were used: r_s = 5.0 nm, σ_s = 1 nm, r_p = 25 nm, $n = 8 \times 10^8$ cm^{-2}, L = 6 μm.

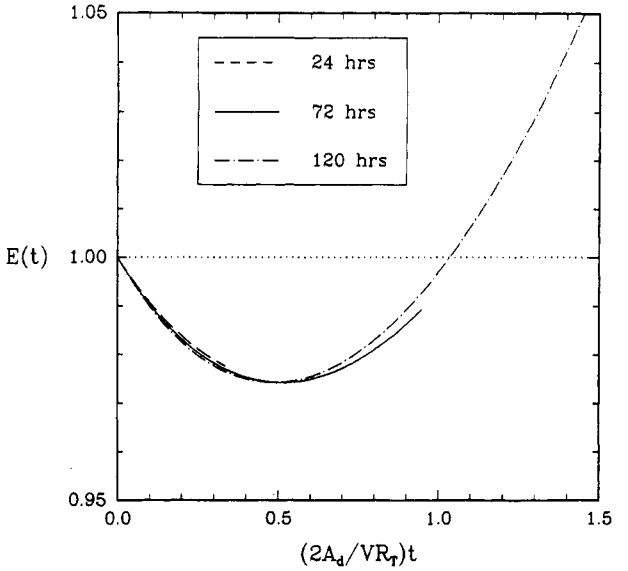

Figure 5. Polydispersity correction term $E(t)$ versus dimensionless time $(2A_d/VR_T)t$ for hindered diffusion runs of 24, 72, and 120 h, sampling concentrations every 4 h. Parameters used are the same as in Figure 4.

PEO,[15] and PVP[16] across the walls of blood capillaries in the kidney are identical with those reported here for the hindered diffusion of these polymers.

The solutions that have been developed for the purely steric partitioning of linear macromolecules[5,27] account only for the loss of conformational entropy of the polymer molecule when it approaches the pore wall. Including an additional polymer–pore interaction, as we have done with the introduction of ε in our model, is typically thought of as including an enthalpic contribution arising from the breakage of polymer–solvent contacts and the formation of polymer–pore contacts. However, in aqueous systems there are a number of other thermodynamic considerations. The solution behavior of many water-soluble polymers, including PEO, PVP, and dextran, is believed to be dominated by the balance of hydrogen bonding and the "hydrophobic effect".[32,33] It is argued that this hydrophobic effect, whereby relatively weak hydration of a solute results in the strengthening of water–water hydrogen bonds, increases the size of short-lived clusters of water in the vicinity of the solute. By use of a variety of techniques,[34-36] dextran, PEO, and PVP have all been shown to have water molecules "bound" to them in free solution. Therefore, there are entropic contributions (due to solvent order), in addition to hydrogen bonding, which affect solution behavior of these polymers.

Solvent structure at the pore wall is another consideration. While there is evidence indicating that the viscosity of water in narrow pores is equal to its bulk value (with the possible exception of a single layer of water molecules at the pore wall),[37] it has been suggested that the structure of water adjacent to a solid surface deviates from its bulk structure more than that of nonpolar solvents. The extent of this additional structure is unclear.[38] In any case, if confinement to a pore alters the ordering of water about the macromolecule (or if the introduction of the polymer alters water structure within the pore), the loss of conformational entropy of the polymer could be offset to some degree by changes in the hydrogen bonding and entropy of the solvent. While this scenario is only speculative, the energy levels (per segment) required to account for the observed behavior of dextran and PVP are comparable to 5% of that of a hydrogen bond. Therefore, the hydrogen bonding and resulting structure of the water are likely to be important considerations in these systems.

Conclusions

The effective diffusion coefficients of the four water-soluble polymers studied decreased with decreasing pore size. While ficoll, a highly cross-linked polymer, diffused at rates comparable to those predicted by the Renkin equation, the diffusion rates of the three linear (or nearly linear) polymers studied differed significantly from those predicted by a theory for noninteracting, linear macromolecules. The hindered diffusion behavior of these linear polymers is consistent with their behavior on SEC columns and can be accounted for by including an additional, thermodynamic polymer–pore interaction in the hindered transport theory for linear macromolecules. Finally, although polydispersity was shown theoretically to have a strong effect on measured hindered diffusion coefficients, the analysis indicates that errors due to polydispersity can be minimized by determining an appropriate duration for the diffusion experiment.

Acknowledgment. We are grateful to Regina Murphy, Jesse Baskir, Roy Hughes, and Brent Mitchell for their valuable assistance in polymer and membrane characterization. We also thank John L. Anderson, Michael P. Bohrer, and Imtiaz Kathawalla for their helpful discussions concerning this work. Glorianne Collver-Jacobson provided expert secretarial assistance. This work was supported by a grant from the National Institutes of Health (DK 20368).

Appendix A. Approximate Expressions for the Hindrance Factors for Noninteracting, Linear Macromolecules

On the basis of a hydrodynamic theory for the hindered transport of flexible, linear macromolecules, we have reported results for the hindrance factor for diffusion, H $(=D/D_\infty)$, and the hindrance factor for convection, W, in tabular form.[3] For convenience in calculations, we have found cubic polynomials which approximate the inverse enhanced drag K^{-1} and lag coefficient G (the hydrodynamic component of W) for the permeability parameter α = 34 and for solute-to-pore size ratios $\lambda \leq 0.87$. The expression

for the inverse enhanced drag is given in eq 4. The corresponding expression for the lag coefficient is

$$G = 1 - 0.0868\lambda - 0.8325\lambda^2 + 0.6737\lambda^3 \quad \text{(A1)}$$

Both of these expressions are accurate to within 2%, and because K^{-1} and G are insensitive to α, they are reasonable approximations for values of α other than 34.

As stated earlier, by combining the inverse enhanced drag with the partition coefficient result of Casassa[5] given in eq 6, the hindrance factor for diffusion can be estimated. It should be noted, however, that for finite polymer chains use of eq 6 (which was developed for chains containing an infinite number of infinitesimally short segments) may lead to substantial underestimates of Φ, especially for large values of λ_g.[27]

By analogy to derivations for solid, spherical solutes[4] we considered the term $\Phi(2 - \Phi)$ as an approximation to the steric exclusion component of the convective hindrance factor. This function was found to be within 7% of results calculated by using a Monte Carlo technique.[3] Therefore, our results for the hindrance factor for convection can be reasonably approximated by using the relation

$$W \approx \Phi(2 - \Phi)G \quad \text{(A2)}$$

where Φ is given by eq 6 and G is given by eq A1.

Appendix B. Effects of Polydispersity

To account for possible polydispersity effects, we have developed the following model, which was used to correct the hindered diffusion data. We assume that the initial polymer mass concentration is normally distributed in solute-to-pore size ratio λ ($=r_s/r_p$), with a mean solute-to-pore size ratio $\bar{\lambda}$ and standard deviation σ ($=\sigma_s/r_p$). The initial concentration of polymer of size ratio λ on the high-concentration side of the membrane, $C_1(\lambda)$, is then given by

$$C_1(\lambda) = \frac{C_{T1}}{(2\pi)^{1/2}\sigma} \exp\left(-\frac{(\lambda - \bar{\lambda})^2}{2\sigma^2}\right) \quad \text{(B1)}$$

where C_{T1} is the total initial concentration on the high-concentration side. The initial concentration on the low-concentration side is assumed to be zero. Assuming that molecules of each size diffuse independently, the concentration of each is governed by eq 9. By integrating over all solute-to-pore size ratios we can express the change in the total mass concentration over time as

$$\ln\left(\frac{\Delta C/\Delta C_0}{E(t)}\right) = -\frac{2A_d}{VR_T(\bar{\lambda})}t \quad \text{(B2)}$$

where ΔC and ΔC_0 refer to total mass concentrations and

$$E(t) = \frac{1}{(2\pi)^{1/2}\sigma}\int_{-\infty}^{\infty} \exp\left(-\frac{(\lambda - \bar{\lambda})^2}{2\sigma}\right) \times \exp\left[\frac{2A_d}{V}\left(\frac{1}{R_T(\bar{\lambda})} - \frac{1}{R_T(\lambda)}\right)\right] d\lambda \quad \text{(B3)}$$

Using the quasi-elastic light-scattering results to estimate $\bar{\lambda}$ and σ and approximating $R_T(\lambda)$ by use of eq 3 and 10, we calculated the correction term $E(t)$ and regressed the hindered diffusion data according to eq B2 to obtain $R_T(\bar{\lambda})$ and thus $D(\bar{\lambda})$. The resulting values of D/D_∞ are those shown in the column of Table IV labeled "corrected".

To consider the effects of polydispersity more generally, we simulated the diffusion of a hypothetical polymer sample which has hindered diffusion behavior governed by the Renkin equation and a solute size distribution given by eq B1. The deviation from the diffusion behavior of a monodisperse sample can be assessed in terms of a residual (Δ) defined as the "actual" value of $\ln(\Delta C/\Delta C_0)$ minus that calculated by linear regression according to eq 9. As an example, Figure 4 shows simulated residuals for diffusion runs of various lengths, with parameters typical of our 15-nm nominal pore radius membranes ($r_s = 5.0$ nm, $\sigma_s = 1$ nm, $r_p = 25$ nm, $n = 8 \times 10^8$ cm^{-2}, and $L = 6$ μm). Figure 5 shows the corresponding polydispersity correction factors $E(t)$. It can be seen that $E(t)$ decreases at short times, reaches a minimum, and then increases to values above unity. Taking concentration readings every 4 h, the error in the measured diffusion coefficient would be +7.6%, +1.0%, and −4.2% for the 24-, 72-, and 120-h runs, respectively. When the degree of polydispersity is greater, $\sigma_s = 2$ nm, the errors in the measured diffusion coefficients increase to +25.1%, −2.4%, and −15.8%, respectively. Therefore, if the length of the diffusion experiment is too short, the effective diffusion coefficient will be overestimated because solutes of smaller size affect the concentration difference disproportionately. This result is in agreement with a polydispersity analysis for short times developed by Kathawalla and Anderson.[12] Furthermore, the small degree of curvature in the residuals for the 24-h run is likely to be masked by other experimental errors, so that examining the residuals would be an insufficient test for polydispersity effects in this case. Allowing the experiment to run too long results in underestimation of the effective diffusion coefficient by placing too much emphasis on the diffusion of larger solutes, which dominates at long times. The simulations suggest that allowing the concentration difference to drop to roughly one-third of its original value minimizes the error due to polydispersity, although this error depends to some degree on the sampling frequency. The magnitude of the errors in D found in these simulations demonstrates the dramatic effect a small degree of polydispersity can have on hindered diffusion results and indicates that choosing an appropriate duration for each diffusion experiment can be useful in minimizing polydispersity effects.

List of Symbols

A	total area of membrane
A_d	exposed membrane area in diffusion cell
A_u	exposed membrane area in ultrafiltration cell
C_1	mass concentration of polymer of a particular size on high-concentration side of membrane
C_{T1}	total mass concentration of polymer on high-concentration side of membrane
ΔC	difference in concentration between the two half-cells
ΔC_0	initial concentration difference between the half-cells
d_i	roots of $J_0(d) = 0$
D	effective diffusion coefficient of macromolecule in membrane, based on external driving force
D_∞	diffusion coefficient of macromolecule in dilute bulk solution
$E(t)$	polydispersity correction term defined by eq B3
G	lag coefficient of solute in a pore
H	hindrance factor for diffusion ($=D/D_\infty$)
k	Boltzmann's constant
K^{-1}	inverse enhanced drag of solute in a pore
L	length of pore
M_n	number-averaged molecular weight
M_w	weight-averaged molecular weight
n	number density of pores in membrane
ΔP	pressure drop across membrane

Q flow rate of solvent across membrane
r_g radius of gyration of a random-coiling macromolecule
r_p radius of pore
r_s Stokes–Einstein radius of macromolecule
R_B boundary layer resistance to mass transfer
R_T total resistance to mass transfer
Sc Schmidt number ($=\eta/\rho D_\infty$)
t time
T absolute temperature
V volume of half-cell in diffusion apparatus
W hindrance factor for convection
W_m mass of membrane

Greek Symbols

α permeability parameter in hindered transport theory for linear macromolecules
Δ residual of ln ($\Delta C/\Delta C_0$), actual minus linear regression
ϵ dimensionless attractive interaction energy between the pore wall and a polymer segment
λ solute-to-pore size ratio based on Stokes–Einstein radius of solute ($=r_s/r_p$)
$\bar{\lambda}$ mean solute-to-pore size ratio λ of a polymer sample
λ_g solute-to-pore size ratio based on solute radius of gyration ($=r_g/r_p$)
Φ partition coefficient of solute between a pore and bulk solution
η solvent viscosity
$[\eta]$ intrinsic viscosity of polymer
ρ density of solvent
ρ_m density of membrane material
σ standard deviation of solute-to-pore size ratio ($=\sigma_s/r_p$)
σ_s standard deviation of Stokes–Einstein radius of polymer

Registry No. PEO, 25322-68-3; PVP, 9003-39-8; ficoll, 25702-74-3; dextran, 9004-54-0.

References and Notes

(1) Anderson, J. L.; Quinn, J. A. *Biophys. J.* **1974**, *14*, 140.
(2) Brenner, H.; Gaydos, L. J. *J. Colloid Interface Sci.* **1977**, *58*, 312.
(3) Davidson, M. G.; Deen, W. M. *J. Membr. Sci.* **1988**, *35*, 167.
(4) Deen, W. M. *AIChE J.* **1987**, *33*, 1409.
(5) Casassa, E. F. *J. Polym. Sci., Polym. Lett. Ed.* **1967**, *5*, 773.
(6) Beck, R. E.; Schultz, J. S. *Biochim. Biophys. Acta* **1972**, *255*, 273.
(7) Wong H., J.; Quinn, J. A. In *Colloid and Interface Science 5*; Kerker, M., Ed.; Academic: New York, 1976; p 169.
(8) Deen, W. M.; Bohrer, M. P.; Epstein, N. B. *AIChE J.* **1981**, *27*, 952.
(9) Bohrer, M. P.; Patterson, G. D.; Carroll, P. J. *Macromolecules* **1984**, *17*, 1170.
(10) Cannell, D. S.; Rondelez, F. *Macromolecules* **1980**, *13*, 1599.
(11) Guillot, G.; Leger, L.; Rondelez, F. *Macromolecules* **1985**, *18*, 2531.
(12) Kathawalla, I. A.; Anderson, J. L. *Ind. Eng. Chem. Res.* **1988**, *27*, 866.
(13) Bohrer, M. P.; Fetters, L. J.; Grizzuti, N.; Pearson, D. S.; Tirrell, M. V. *Macromolecules* **1987**, *20*, 1827.
(14) Bohrer, M. P.; Deen, W. M.; Robertson, C. R.; Troy, J. L.; Brenner, B. M. *J. Gen. Physiol.* **1979**, *74*, 583.
(15) Jorgensen, K. E.; Moller, J. V. *Am. J. Physiol.* **1979**, *236*, F103.
(16) Vanrenterghem, Y.; Vanholder, R.; Lammens-Verslijpe, M.; Lambert, P. P. *Clin. Sci.* **1980**, *58*, 65.
(17) Provencher, S. W. *Makromol. Chem.* **1979**, *180*, 201.
(18) Mitchell, B. D.; Deen, W. M. *J. Colloid Interface Sci.* **1986**, *113*, 132.
(19) Schultz, J. S.; Valentine, R.; Choi, C. Y. *J. Gen. Physiol.* **1979**, *73*, 49.
(20) Malone, D. M.; Anderson, J. L. *AIChE J.* **1977**, *23*, 177.
(21) Colton, C. K.; Smith, K. A. *AIChE J.* **1972**, *18*, 958.
(22) Long, T. D.; Jacobs, D. L.; Anderson, J. L. *J. Membr. Sci.* **1981**, *9*, 13.
(23) Stuart, M. A. C.; Cosgrove, T.; Vincent, B. *Adv. Colloid Interface Sci.* **1986**, *24*, 143.
(24) Kim, J.-O.; Anderson, J. L. Presented at the AIChE Annual Meeting, New York, 1987; paper 5j.
(25) Idol, W. K.; Anderson, J. L. *J. Membr. Sci.* **1986**, *28*, 269.
(26) Yavorsky, D. P. Ph.D. Thesis, University of Pennsylvania, 1981.
(27) Davidson, M. G.; Suter, U. W.; Deen, W. M. *Macromolecules* **1987**, *20*, 1141.
(28) Callaghan, P. T.; Pinder, D. N. *Macromolecules* **1983**, *16*, 968.
(29) Rossi, C.; Bianchi, E.; Conio, G. *Chem. Ind. (Milan)* **1963**, *45*, 1498.
(30) Scholtan, W. *Makromol. Chem.* **1952**, *7*, 209.
(31) Bellenkii, B. G.; Vilenchik, L. Z.; Nesterov, V. V.; Kolegov, V. J.; Frenkel, S. YA. *J. Chromatogr.* **1975**, *109*, 233.
(32) Burchard, W. In *Chemistry and Technology of Water-Soluble Polymers*; Finch, C. A., Ed.; Plenum: New York, 1983; pp 125–142.
(33) Franks, F. In *Chemistry and Technology of Water-Soluble Polymers*; Finch, C. A., Ed.; Plenum: New York, 1983; pp 125–142.
(34) Gekko, K. In *Solution Properties of Polysaccharides*; Brant, D., Ed.; ACS Symposium Series 150; American Chemical Society: Washington, DC, 1981; pp 415–438.
(35) Molyneux, P. In *Water: A Comprehensive Treatise*; Frank, F., Ed.; Plenum: New York, 1975; pp 569–757, Vol. 4.
(36) Maxfield, J.; Shepherd, I. W. *Polymer* **1975**, *16*, 505.
(37) Anderson, J. L.; Quinn, J. A. *J. Chem. Soc., Faraday Trans. 1* **1972**, *68*, 744.
(38) Clifford, J. In *Water: A Comprehensive Treatise*; Frank, F., Ed.; Plenum: New York, 1975; Vol. 5, pp 75–132.